

# ESTIMATION OF RADIOMETRIC CALIBRATION COEFFICIENTS FOR RESOURCESAT-2 (RS-2) LISS-3 SENSOR USING GROUND BASED TARGETS

Raghavender.N , Santhi Sree.B, Raju.K.S., Chandrasekaran. D, Gopala Krishna.B  
Data and Product Quality Evaluation Division, Satellite Data Product Quality Assurance Group, Data Processing  
Products Archival and Web Applications Area, National Remote Sensing Centre, Balanagar, Hyderabad-500037  
(Email: santhisree\_b@nrsc.gov.in)

**KEYWORDS:** Vicarious Calibration; Resourcesat-2; Cal/Val site; Shadnagar; 6S model

**ABSTRACT:** Radiometric calibration of sensors is an important activity performed by remote sensing data providers to ensure accurate and reliable data products. The current work describes the post launch radiometric calibration of Resourcesat -2 (RS-2), Linear Imaging Self Scanner-3 (LISS-3) sensor operated in four bands: 0.52-0.59  $\mu\text{m}$ , 0.63-0.69  $\mu\text{m}$ , 0.77-0.86  $\mu\text{m}$  and 1.55-1.7  $\mu\text{m}$  with a spatial resolution of 23.5m over very well maintained targets in Calibration/Validation (Cal/Val) site in Shadnagar. The calibration coefficients were computed using the satellite image data sets acquired between January 2015 and April 2017. The radiances obtained from sensor were compared with simulated satellite radiances using 6S Radiative Transfer (RT) code, whose inputs are ground measured surface reflectance in sensor spectral response, synchronous Aerosol Optical Depth (AOD) measurements, Ozone and Water Vapor measurements. Mathematical relation is modeled for the LISS-3 Digital Numbers (DN), simulated radiances and band wise calibration coefficients were obtained. Calibration coefficients applied on the validation data sets show considerable improvement and an overall agreement of better than 5% with Landsat-7 (L7) Enhanced Thematic Mapper plus (ETM+) and Landsat8 (L8) Optical Land Imager (OLI) .

## 1. INTRODUCTION

Data products generated with earth observation sensor data are expected to be highly accurate and radiometrically stable during its operational phase in orbit. In order to derive reliable information from the products, the calibration coefficients supplied along with the products to convert the DN into physical units (like radiance, reflectance) should be monitored and fine tuned on regular basis. Conversion of DN to radiance is arrived using Equation 1. Calibration coefficients derived in the laboratory prior to the launch are traceable to well known standards such as National Institute of Standards and Technology (NIST) are subjected to change after launch. The possible factors which influence the performance of the sensor system are: deep space environment, launch stresses etc (Thome, 2001).

$$L = (\text{Gain} \times \text{DN}) + \text{Offset} \quad (1)$$

Where  $\text{Gain} = (L_{\text{max}} - L_{\text{min}}) / \text{DN}_{\text{max}}$ ,  $\text{Offset} = L_{\text{min}}$ ,  $L$  is the spectral band radiance in units of  $\text{mW} \cdot \text{cm}^{-2} \cdot \text{sr}^{-1} \cdot \mu\text{m}^{-1}$ ,  $L_{\text{min}}$  and  $L_{\text{max}}$  are the minimum and maximum spectral band radiance respectively and  $\text{DN}_{\text{max}}$  is the maximum DN depending on the quantisation bits (for 10 bits quantisation,  $\text{DN}_{\text{max}} = 2^{10} - 1 = 1023$ ). Gain and Offset as a set are called as calibration coefficients

Post-launch sensor performance is monitored essentially through extensive Cal/Val activities. Vicarious calibration is an independent approach (Dingirard, 1999, Biggar, 2003, De Vries, 2007, Mishra 2014,) which refers to the process of determining sensor calibration coefficients using synchronously collected field measurements (includes radiance/reflectance, atmospheric parameters) with satellite pass and the sensor DN of the same area. This approach majorly relies on homogeneous test site, accurate field instruments and good RT code for the calibration. Calibration coefficients so obtained be verified with the current ones and the corrections can be implemented based on the requirement.

Resourcesat-2 (RS-2) satellite was launched by Polar Satellite Launch Vehicle (PSLV-C16) on 20April, 2011 with onboard sensors: LISS - 4, LISS - 3 and Advanced Wide Field Sensor (AWiFS). It is a global continuity mission similar to Resourcesat-1 (RS-1 or IRS-P6) satellite, with enhanced features for integrated land and water resources management. Major specifications of RS-2 sensors are included in Table 1 (NRSC, 2011).

The current work estimates the calibration coefficients through the vicarious calibration approach for the four bands of LISS-3 sensor using two different intensity level artificial targets present in National Remote Sensing Centre (NRSC)-Shadnagar campus. Coefficients obtained were applied on LISS-3 data sets and verified with ETM+ and OLI data sets.

Table 1 Major specifications of Resourcesat-2 sensors

Parameter	LISS-4	LISS-3	AWiFS
Spatial Resolution in across track direction at nadir (m)	5.8	23.5	56.0
Swath (km)	70	141	740
Spectral Bands (microns)	Band2 (B2): 0.52-0.59 Band3 (B3): 0.62-0.68 Band4 (B4): 0.77-0.86	Band2 (B2): 0.52-0.59 Band3 (B3): 0.62-0.68 Band4 (B4): 0.77-0.86 Band5 (B5): 1.55-1.70	Band2 (B2): 0.52-0.59 Band3 (B3): 0.62-0.68 Band4 (B4): 0.77-0.86 Band5 (B5): 1.55-1.70
Saturation Radiance (mW.cm <sup>-2</sup> .sr <sup>-1</sup> .μm <sup>-1</sup> )	B2:52 B3:47 B4:31.5	B2:52 B3:47 B4:31.5 B5:7.5	B2:52 B3:47 B4:31.5 B5:7.5
SNR @saturation	>128		>512
Quantisation (Bits)	10 (7bit data is transmitted to BDH after DPCM)		12 (10 bit transmission after MLG)
No.of gains	Single gain (100% albedo)		

## 2. STUDY AREA

Indian Space Research Organisation (ISRO) has setup an artificial test site (refer Figure 1) for vicarious calibration at NRSC-shadnagar and made operational in January 2016, after fully characterizing the targets and atmospheric profiles for a period of two years. It caters to the calibration of earth observation sensors (EOS) operating in visible, near infrared region (VNIR) with spatial resolutions better 25m. Site is geographically located at 17.034° N latitude, 78.184° E longitude and altitude of 630m. It is spread in a sprawling area of ~250m X 250m. Site is divided into eight blocks and filled with five natural target materials (Black Stone, Black Soil, Gravel, Red Soil and White Stone) with reflectance ranging from 7% to more than 50%. These five discrete reflectance levels are useful for sensor radiometric characterization at five different levels and the contrast between black and white stone is useful for determining edge based point spread function (PSF) and modulation transfer function (MTF) of the sensor. A strong subsoil drainage network was laid beneath the surface to prevent upper soil erosion due to rainfall. Apart from the eight blocks, a concrete strip of 103m X 21m (in the left most end in Figure 1) was also built to characterize high spatial resolution sensors better than 1m. Detailed dimensions of individual blocks are provided in Table 2.

Table 2 Target materials and their dimensions

Target Material	Reflectance (%) in NIR band	Target Size in meters (LXW)	No. of blocks
Black Stone (A)	7	70 X 70	02
Black cotton soil (B-1)	9	125 X 105	01
Black cotton soil (B-2)	9	140 X 50	01
Grey stone/Gravel (C)	18	140 X 50	01
Red Soil (D)	26	125 X 105	01
White Stone (E)	69	70 X 70	02
Painted concrete strip	-----	103 X21	01

Best time to conduct field experiments in shadnagar site is between January to April, November to December in a calendar year. During this time period of six months sky is relatively cloud free and targets are maintained vegetation free and good condition. Variation in few important atmospheric parameters like AOD at 550nm, water vapor and ozone is 0.2 to 0.6, 0.4 to 2cm and 240-330DU respectively.

Black soil (B-1) and red soil (D) targets were selected for LISS-3 sensor calibration based on the suitable dimensions for LISS-3 resolution. LISS-3 sensor images the two targets each in ~5 X 4 pixels, however only 3 X 2 pixels were considered as pure pixels leaving out one pixel all around for adjacency effects. Pure pixels on both the

targets are shown in Figure 2. It is observed that the pixels identified under “pure” were having less standard deviation in comparison to the total (5X4) pixels. This phenomenon arises purely due to the sensor sampling of the target.

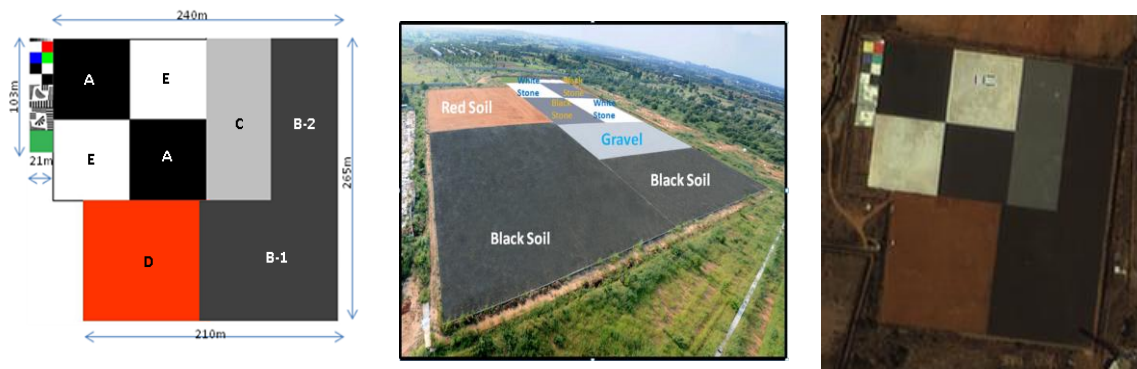


Figure 1 Calibration site layout (left), Field photograph (middle), site as viewed by an ISRO's high resolution sensor (right).

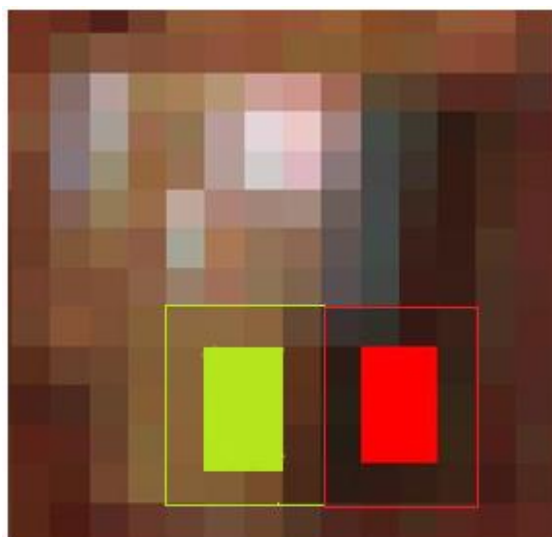


Figure 2 A sample LISS-3 image with highlighted black and red soil targets. The outline indicates the total pixels (5X4) and the solid fill shows the pure pixels in each target. Black, Red soils are indicated in red, green colours respectively.

### 3. SATELLITE DATA

Satellite data sets acquired over the study area between January 2015 and April 2017 were considered for calibration and validation. Though the site was officially declared operational in January 2016, data sets acquired prior to it were also included to have larger dataset size. Altogether three different satellite data sets were utilized in the study. RS2-LISS-3 data sets for calibration, L7-ETM+ and L8-OLI data sets for validation. Standard Geo-referenced products (with UTM projection and WGS84 datum) from the operational data processing chain for three sensors were used for the analysis. Level-1T data sets of ETM+ and OLI were downloaded from Earth Explorer website (USGS website).

#### 3.1 Spectral response functions of RS2-LISS3, L7-ETM+ and L8-OLI

The spectral response functions (SRF) of four RS2-LISS3 bands and equivalent bands of L7-ETM+ and L8-OLI (source: USGS website) sensors are given in Figure 3. Spectral bands of L7-ETM+ and L8-OLI sensors (source: respective handbooks) are provided in Table 3. It is observed that B2, B3 of LISS3 closely match, where as B4, B5 of LISS3 show significant differences with equivalent bands of ETM+ and OLI. The maximum percentage disagreement (PDA) between LISS-3 and ETM+ bands calculated in terms of band integrated surface reflectance is 3% in B3 and less than 1% in other bands. Similarly with OLI bands it is maximum 2 % in B2 and less than 1% in other bands.

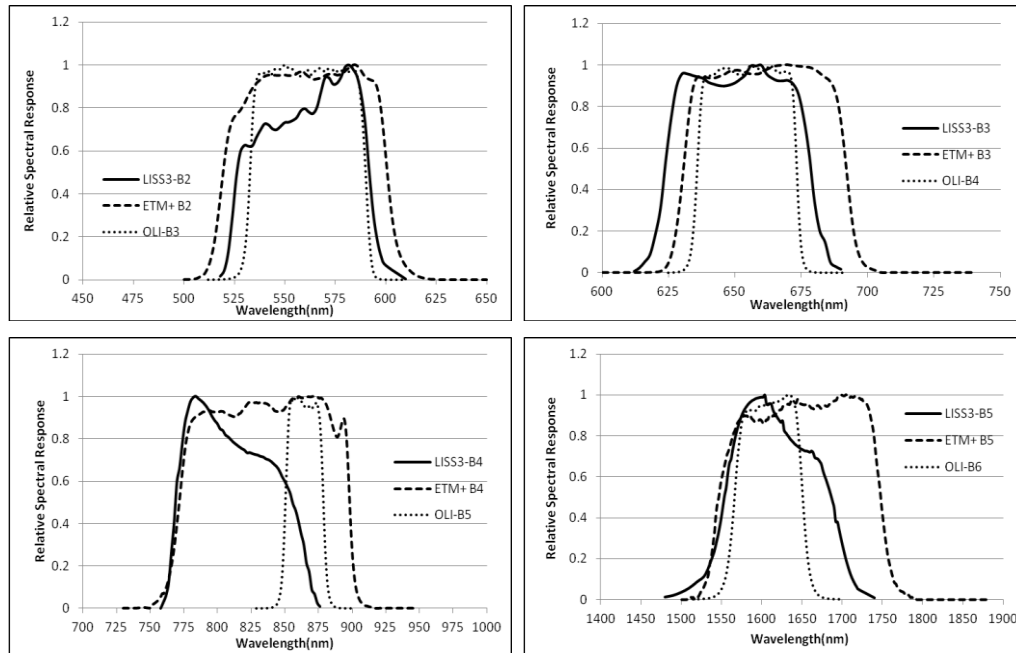


Figure 3 SRF of LISS-3 with corresponding bands of ETM+ and OLI.

### 3.2 Calibration dataset

A total of six dates (28-Jan-15, 12-Nov-15, 16-Feb-16, 22-May-16, 10-Feb-17 and 30-Mar-17) comprising two dates from each year for three consecutive years (2015-2017) were selected for calibration. Site is covered in path-100, row -61 of Resourcesat referencing scheme with scene center time around 5:30 Hrs GMT. Selected dates with solar angles and other information are given in Table 4.

### 3.3 Validation dataset

Calibration coefficients obtained were applied on independent datasets of LISS-3 and in turn validated with ETM+ and OLI sensor data sets. These two Landsat sensors acquire the site with one day gap and at nearly same time of the day that of LISS-3. Site is covered in path-144, row -48 of World Referencing Scheme (WRS) -2 for both ETM+, OLI sensors, with scene center time around 5:10 Hrs GMT. Details of the validation pairs are given in Table 5 and 6. We could get a total of seven near simultaneous acquisitions over the site, three with ETM+ sensor and four with OLI sensor.

## 4. FIELD MEASUREMENTS

Primary field measurements sufficient to simulate the atmospheric conditions and there by estimate the at-sensor radiance are AOD, ozone (O<sub>3</sub>) concentration, water vapor (WV) and surface reflectance. Instruments employed to measure these parameters were sunphotometer (make: CIMEL, France), MicroTOPS ozone monitor (make: Solar Light, USA) and spectroradiometer (make: Spectra Vista Corporation, USA). Sunphotometer measures AOD in nine discrete wavelengths between 340-1640nm, Ozone concentration was derived using measurements at three UV wavelengths, columnar water vapor was derived using measurements at two NIR wavelengths and the surface reflectance was measured in 350-2500nm wavelength region.

Field measurements were carried out for one hour duration, starting half an hour before the satellite pass time (w.r.t. scene center time) and continuing upto half an hour after the satellite pass time. Sunphotometer measurements were done at 15minute interval and O<sub>3</sub>, WV were done at 5 minute interval. While the surface reflectance measurements were done by carrying the spectroradiometer to each of the target types (black and red soil). They were made along the North-South and South –North directions in continuous mode. A total of 20 observations were collected in the pure pixels area of each target type. Average of the multiple measurements was input to RT code. Mean surface reflectance of two targets (black and red soil) for six dates in LISS-3 bands is shown in Figure 4. Standard deviation is <2 %, <3% on black soil, red soil respectively. Atmospheric parameters measured on six dates are tabulated in Table 7.

Table 3 Spectral bands of L7-ETM+, L8-OLI sensors

Sensor	Bands (in $\mu\text{m}$ )	Spatial Resolution (m)	Swath (km)
L7-ETM+	B1(0.450-0.515)	30	185
	B2(0.525-0.605)		
	B3(0.630-0.690)		
	B4(0.775-0.900)		
	B5(1.550-1.750)		
	B6(10.40-12.50)	60	
	B7(2.090-2.350)	30	
	PAN(0.52-0.90)	15	
L8-OLI	B1(0.435-0.451)	30	190
	B2(0.452-0.512)		
	B3(0.533-0.590)		
	B4(0.636-0.673)		
	B5(0.851-0.879)		
	B6(1.566-1.651)		
	B7(2.107-2.294)		
	B8 / PAN (0.503-0.676)	15	
	B9(1.363-1.384)	30	
	B10(10.60-11.19)	100	
	B11(11.50-12.51)	100	

Table 4 Calibration data (LISS-3) scene details

Experiment date	Path-Row	Scene Center time (GMT in hh : mm : ss)	Solar Elevation angle (deg)	Solar Azimuth angle (deg)
28-Jan-15	100-61	05:23:12	47.89	145.13
12-Nov-15		05:25:00	52.19	154.40
16-Feb-16		05:26:18	52.77	140.28
22-May-16		05:27:02	71.80	75.14
10-Feb-17		05:27:15	51.51	142.29
30-Mar-17		05:27:00	65.88	119.93

Table 5 Details of LISS-3/ETM+ validation sets

Date of Pass	Sensor	Path-Row	Scene Center time (GMT in hh:mm:ss)	Solar Elevation angle (deg)	Solar Azimuth angle (deg)
23-Jan-16 / 24-Jan-16	LISS-3 / ETM+	100-61 / 144-48	05:26:04 ./ 05:11:24	47.37 / 44.79	147.41 / 143.03
28-Apr-16 / 29-Apr-16			05:26:52 / 05:12:02	71.51 / 67.64	94.86 / 93.71
24-Dec-16 / 25-Dec-16			05:27:28 / 05:12:02	45.62 / 43.10	154.12 / 149.50

## 5. METHODOLOGY

### 5.1 Generation of calibration coefficients

Here in the present work reflectance based vicarious calibration approach (Thome, 2001) was followed. In this approach RS2 LISS-3 at-sensor radiance was estimated using surface reflectance and atmospheric parameters as inputs to 6S (Vermonte, 2006) RT code. Flow chart describing the approach is shown in Figure 5. Calibration coefficients were computed by utilizing the six LISS-3 datasets and field measurements as listed in Table 4 and 7.

Table 6 Details of LISS-3/OLI validation sets

Date of Pass	Sensor	Path-Row	Scene Center time (GMT in hh:mm:ss)	Solar Elevation angle (deg)	Solar Elevation angle (deg)
04-Apr-16 / 05-Apr-16	LISS-3 / OLI	100-61 / 144-48	05:26:45 / 05:09:18	67.25 / 63.09	116.09 / 111.34
17-Jan-17 / 18-Jan-17			05:27:21 / 05:09:49	46.78 / 43.86	149.13 / 144.00
06-Mar-17 / 07-Mar-17			05:27:09 / 05:09:28	58.55 / 54.97	133.28 / 127.67
23-Apr-17 / 24-Apr-17			05:26:48 / 05:09:02	70.88 / 66.39	99.81 / 97.45

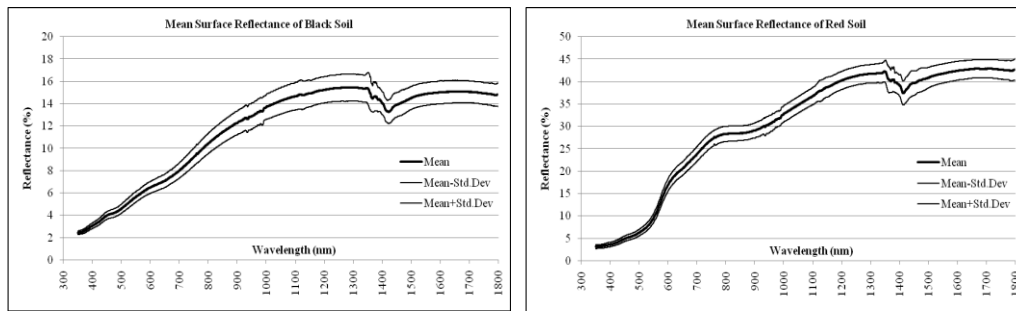


Figure 4 Mean surface reflectance of black and red soil in LISS-3 bands.

**Sequence of steps involved in the process:**

*Step1:* Average surface reflectance was computed out of 20 measurements of a target (as discussed in section 4) and resampled to 1nm interval.

*Step2:* Mean reflectance obtained in step1 was weighted with LISS-3 band SRF (at 1nm interval) and band integrated reflectance was computed using below equation

$$\langle \rho_k(\lambda) \rangle = \frac{\int \rho(\lambda) SRF_k(\lambda) d\lambda}{\int SRF_k(\lambda) d\lambda}$$

*Step3:* Mean of all the measurements (AOD, O3 and WV) collected for one hour duration was computed. Refer Table 7.

*Step4:* Solar zenith and azimuth angles, view zenith and azimuth angles and satellite height were picked from the data product.

*Step5:* At-sensor spectral band radiance was simulated by supplying parameters obtained in steps 2 to 4, wavelength limits (lower and higher), aerosol model as continental, surface type as lambertian and target height, as inputs to 6S.

*Step6:* Calibration coefficients were estimated for a band considering mean DN<sub>s</sub> for different targets in the LISS-3 image and their corresponding simulated radiance. Here in the present work only two targets were considered and hence the coefficients were computed based on these two targets only.

*Step7:* Steps 2, 5, 6 were repeated to estimate coefficients for other bands.

Table 7 Atmospheric parameters

Experiment date	Mean AOD at 550nm	Mean Ozone (DU)	Mean Water vapor (cm)
28-Jan-15	0.203	265.91	0.68
12-Nov-15	0.577	316.44	1.65
16-Feb-16	0.317	245.76	1.24
22-May-16	0.348	296.60	1.50
10-Feb-17	0.566	286.00	1.00
30-Mar-17	0.603	328.34	1.09

## 5.2 Validation of LISS-3 radiance with ETM+ and OLI

Calibration coefficients estimated in the section 5.1 were applied on LISS-3 datasets and the new LISS-3 sensor radiances were validated with ETM+, OLI sensor radiances. Refer Table 5 and 6 for the list of dates. Since ETM+ and OLI sensor spatial resolutions are coarser than LISS-3, only 2X2 pure pixels area was considered for further analysis. Two targets identified in OLI image is shown in Figure 6. Mean DN of four pixels was calculated for each target and was converted to radiance using the coefficients supplied along with the product in the metafile. The radiance obtained on two targets with new coefficients of LISS-3 using Equation 1 was compared with corresponding ETM+ / OLI pair and the PDA was noted.

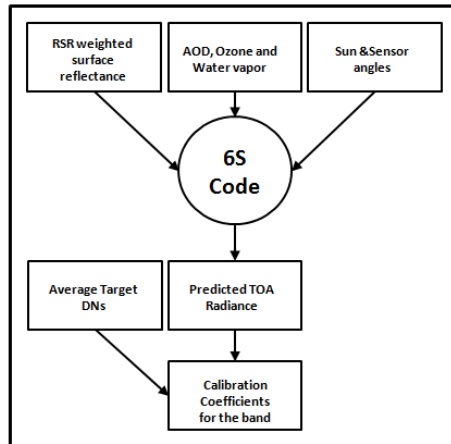


Figure 5 Reflectance based vicarious calibration flow chart.

## 6. RESULTS AND DISCUSSIONS

LISS-3 sensor radiance and 6S simulated radiances for all six calibration data sets are tabulated in Table 8 and the same are plotted against each other in Figure 7. It can be observed clearly that, as the radiance values are increasing the linear fit line is deviating from the linear (one-one) line. This indicates that the errors are increasing with increase in radiance. Calibration coefficients were worked out from LISS-3 DNs and corresponding 6S radiance by a mathematical model. New coefficients derived are tabulated in Table 9 along with the old coefficients.



Figure 6 Two targets identified in L8-OLI image. “Pure pixels” are filled with solid color, “red” for red soil and “green” for black soil. Outline line shows the total pixels for each target type.

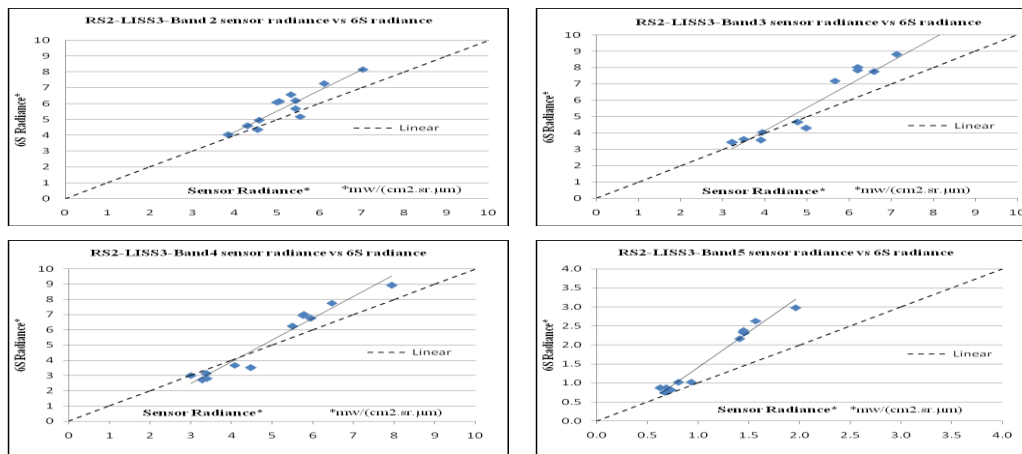


Figure 7 Agreement between LISS-3 and 6S radiance for calibration data sets.

Table 8 LISS-3 and 6S simulated radiances

Date of Experiment	LISS-3 Bands	Black Soil		Red Soil	
		Sensor Radiance	6S Radiance	Sensor Radiance	6S Radiance
28-Jan-15	B2	3.846	4.033	5.006	6.085
	B3	3.216	3.422	6.194	7.849
	B4	3.007	3.002	5.773	7.033
	B5	0.629	0.867	1.447	2.332
12-Nov-15	B2	4.303	4.591	5.057	6.127
	B3	3.491	3.622	5.658	7.189
	B4	3.274	2.699	5.501	6.236
	B5	0.672	0.754	1.406	2.163
16-Feb-16	B2	4.540	4.356	5.430	6.177
	B3	3.897	3.553	6.585	7.752
	B4	3.402	2.801	5.947	6.759
	B5	0.733	0.815	1.454	2.313
22-May-16	B2	5.540	5.178	7.023	8.157
	B3	4.984	4.290	8.744	10.257
	B4	4.480	3.514	7.944	8.917
	B5	0.929	1.020	1.959	2.977
10-Feb-17	B2	4.575	4.942	5.320	6.564
	B3	3.936	4.044	6.210	8.027
	B4	3.377	3.141	5.763	6.941
	B5	0.690	0.869	1.446	2.378
30-Mar-17	B2	5.430	5.672	6.108	7.259
	B3	4.778	4.671	7.121	8.811
	B4	4.080	3.671	6.461	7.755
	B5	0.805	1.016	1.568	2.628



Table 9: Gain and offset for each band

LISS-3 Bands	Gain <sub>new</sub>	Offset <sub>new</sub>	Gain <sub>old</sub>	Offset <sub>old</sub>
B2	0.0664	-1.0729	0.0508	0
B3	0.0584	-0.7321	0.0459	0
B4	0.0371	-0.5705	0.0308	0
B5	0.0120	-0.2119	0.0073	0

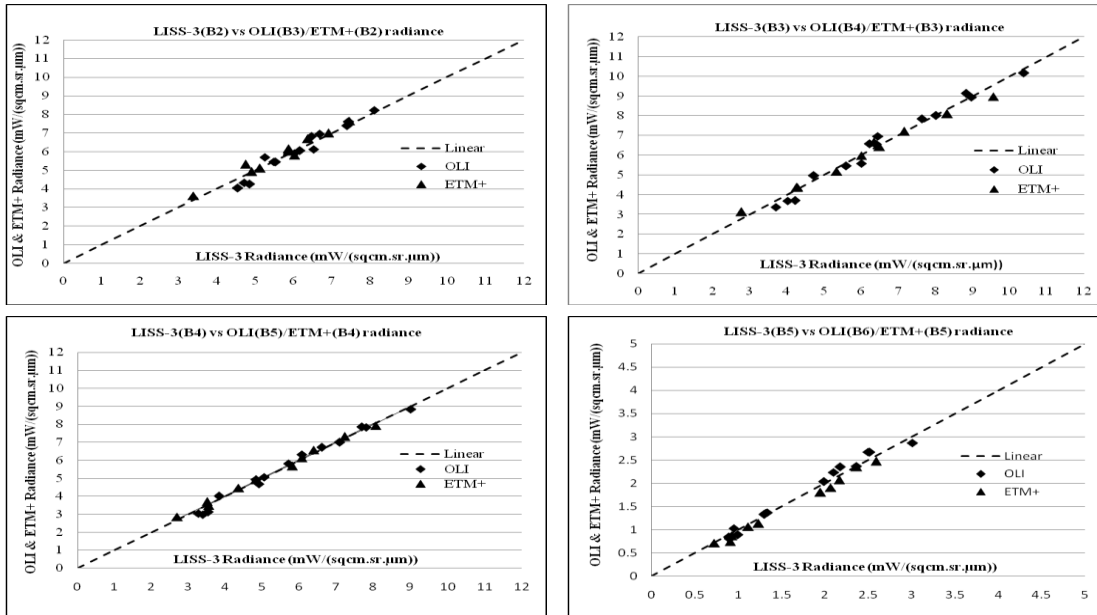


Figure 8 Comparison of new LISS-3 radiances with ETM+ and OLI radiances.

New coefficients thus obtained (in Table 9) were applied on LISS-3 validation data sets to get calibrated radiances. The new LISS-3 radiances were compared with ETM+ and OLI radiances. Comparison plots are shown in Figure 8. Maximum sun elevation difference between LISS-3 and ETM+/OLI acquisition dates is less than 5deg. Influence of this sun angle difference on sensor radiance is less than 0.5%. The PDA of LISS-3 radiance was better than 2.5%, 2%, 1%, 5%, in B2, B3, B4, B5 bands respectively with ETM+ sensor. Similarly with OLI the PDA was better than 1%, in B2-B4, and 2.5 % in B5.

## 7. CONCLUSIONS

Based on the present work following are the conclusions:

- Calibration coefficients for all bands of LISS-3 are derived and its in the process of implementation in the data processing chain for the information of user community.
- Artificial targets present in the Cal/Val site are promising for vicarious sensor calibration/validation.
- The radiometric accuracy with the new calibration coefficients results into better than 10% . The relative radiometric accuracy compared to OLI results into better than 3% and with ETM+ results into better than 5%.
- The effective calibration coefficients derived based on six calibration datasets holding well and in agreement with the other dates of acquisitions over the same targets.

**Future scope of work:** Present study using soil targets of ISRO site over different acquisitions will provide calibration coefficients in the dynamic range from 12% to 45% for Band2 to Band5. As the availability of high reflectance targets like snow, salt pans are season based and inaccessible for periodical observations, hence commonly available soil targets were opted for the deployment in the site. The study using the ISRO site is limited in this dynamic range. Internationally, sand feature based deserts or dry lake beds are the most common targets used for vicarious calibration exercise as they are pseudo invariant. The ‘Red Soil’ spectral trend is similar to desert

sand. However, the response could be 15% to 20% higher to 'red soil' response for the standard deserts like Libya or Algeria. The vicarious calibration experiments conducted over Rajasthan desert during January 2017 results are closely matching with ISRO site experiment results. So the calibration coefficients derived using this well maintained site are more realistically matching upto the dynamic range covered by most of the targets. There could be different deviations with reference to high reflectance targets. This could be confirmed only by conducting experiments over high reflectance (snow) targets.

## **8. ACKNOWLEDGEMENTS**

Authors are grateful to Dr. Y.V.N.Krishna Murthy, Director, NRSC, for his guidance and encouragement during this work. We are thankful to RS2 intercenter Project, Mission , Operations teams and CMG.NRSC for the timely support with products/services. Our special thanks are due to Dr. A. Senthil Kumar, Director IIRS and former Group Director( G&SPG/SDAPSA/NRSC) for his significant contributions while establishing this facility in NRSC.

## **REFERENCES**

### **References from Journals**

- Biggar, S.F.; Thome, K.J.; Wisniewski, W, 2003. Vicarious radiometric calibration of EO-1 sensors by reference to high-reflectance ground targets. *IEEE Trans. Geosci. Remote Sens.*, 41, pp 1174–1179.
- De Vries, C., T. Danaher, R. Denham, P.Scarth, and S.Phinn, 2007. An operational radiometric calibration procedure for Landsat sensors based on pseudo-invariant targets. *Remote Sensing of Environment*, 107, pp. 414-429.
- Dinguirard, M., and P.N.Slater, 1999. Calibration of space multi-spectral imaging sensors: A review. *Remote Sensing of Environment*, 68, pp. 194-205.
- Mishra, N.; Helder, D.L.; Angal, A.; Choi, T.; Xiong, X., 2014. Absolute calibration of optical satellite sensors using Libya 4 pseudo invariant calibration site. *Remote Sensing*, 6, pp 1327–1346.
- Thome , K. J., 2001. Absolute radiometric calibration of Landsat-7 ETM+ using the reflectance based method. *Remote Sensing of Environment*, 78, pp. 27-38.
- Vermonte, E., D.Tanre, J.L.Deuze, M. Herman, J.J.Morcrette, and S.Y.Kotchenova, 2006. Second Simulation of Satellite Signal in Solar Spectrum(6S). 6S User guide version3, University of Maryland.

### **References from Other literature**

- NASA, Landsat 7 Science Data Users Handbook
- NASA, 2016, Landsat 8 Data Users Handbook, Version 2.0.
- NRSC, 2011. Resourcesat-2 Data User's Handbook

### **References from websites**

- United States Geological Survey. Available online:<https://landsat.usgs.gov/using-usgs-spectralviewer>
- United States Geological Survey. Earth Explorer. Available online:[www.earthexplorer.usgs.gov](http://www.earthexplorer.usgs.gov)